THE ASTROPHYSICAL JOURNAL, 233:799–808, 1979 November 1

STRUCTURE WITHIN REDSHIFT-MAGNITUDE BANDS, MORPHOLOGICAL EVOLUTION[1]

WILLIAM G. TIFFT
Steward Observatory, University of Arizona
Received 1978 August 15; accepted 1979 May 10

ABSTRACT

The distribution of redshifts within individual redshift-magnitude bands contains a significant periodic structure of "X-groups" which cross the bands at a steep angle. Six independent cluster samples indicate that the pattern appears to be fixed in redshift and magnitude. Five compact E-dominated groups of galaxies are superposed and shown to concentrate at the boundaries between X-groups. Morphology is shown to be ordered across X-groups, suggesting evolutionary sequences linking groups. All correlations are demonstrated with several independent data samples.

Subject headings: galaxies: photometry — galaxies: redshifts

I. INTRODUCTION

In recent papers (Tifft 1978*b*, hereafter BT; Tifft and Gregory 1979, hereafter CS) the existence of redshift-magnitude bands and their possible relationship to galaxy evolution have been refined. Substructure in the redshift and morphological distributions within bands has not been discussed. However, if the bands represent evolutionary structures, some regularity would be expected. The organization need not be simply a separation in mean redshift by morphology, but it should present a significant repeatable pattern.

Preliminary concepts of bands from BT provide guidelines for an internal study of individual bands. Galaxies are hypothesized to arise from expansion of individual singularities. The injection-point redshift depends upon cosmic time, shifting generally toward lower redshift with time. One aspect of this paper will be to examine the hypothesized injection process, whether continuous along bands or limited to specific points. A second hypothesis is that there is a general time-morphological trend within individual galaxies. Early elliptical morphology is hypothesized to trend toward nonelliptical types. We will use this concept as a means of estimating relative time since emergence. As in CS, we will consider compact groups of ellipticals as recently emerged, well-developed clusters with mixed morphology as intermediate, and diffuse spiral-dominated populations as most advanced. Morphological evolution, coupled with the drift of injection toward lower redshift, leads naturally to the general trend of morphology along bands. There are, however, peculiarities and regularities which suggest finer structure.

Two types of fine structure relating to bands have been introduced previously. The finest structure, the "discrete redshift" (Tifft 1978*a*, with earlier references) will not be a major concern of this paper. A coarser structure, originally introduced (Tifft 1973*a*) under the name "spin groups," will be considered in detail. To minimize interpretations, we shall rename the substructures X-groups. We shall (1) discuss their existence; (2) examine possible relationships to galaxy injection; and (3) examine their association with morphology. We shall be concerned primarily with the two brightest Coma bands, denoted CU (upper) and CM (middle), and in most cases will use m_p magnitudes from the CGCG catalog of Zwicky *et al.* (1960–1968, hereafter CGCG).

II. X-GROUPS AND THE CU BAND

X-groups were first defined (Tifft 1973*a*) using redshifts and nuclear magnitudes in Coma. Figure 1 shows the groups using the most recent data. No previous statistical analysis has been done beyond noting that a disturbance, indicative of structure, appears in power spectra when redshift-magnitude diagrams are projected at steep slopes (Tifft 1973*a*, *b*). The slope of X-groups in Coma $V(4.8)$ nuclear magnitude diagrams is $q \approx 9$ (all slopes in this paper are expressed in magnitudes per factor of 2 in redshift). The nuclear magnitude band slope for Coma is $s \approx 3.25$, while for galaxy total magnitudes or QSS magnitudes $s \approx 4.28$. We can predict q for total magnitudes by assuming the q scales like s in going from nuclear to total magnitudes. Thus $q \approx 12$ is close to what we would expect. A more precise figure is not warranted or necessary, since in general the groups are quite short. Since to first order q is predictable, it is not an arbitrary variable in the discussions which follow. In fact, virtually all quantities involved are fixed. Specific

[1] After an extensive independent statistical analysis, the referee could not demonstrate that the bands discussed in this and previous papers do not exist, but he was also not convinced by the author's analyses that the bands and cross-bands do exist. In this stalemate on a question of possible considerable importance, we will permit the author to present his evidence in hopes that an open forum will encourage research and a resolution of this disagreement.—ED.

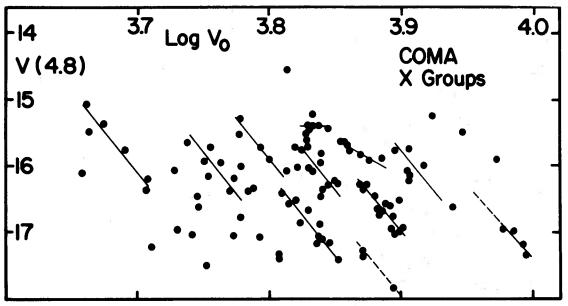

FIG. 1.—X-groups as presently identified in the Coma cluster.

locations of bands for total magnitudes are given in BT. With new samples we will automatically assign galaxies to the "nearest band" for statistical purposes. One exception to this rule applies to galaxies above the CU band which might belong to the Q6 band. The Q6 band is at present too poorly defined to determine membership accurately for the few galaxies involved.

The statistical index we will use to define X-groups is the redshift, V_x, projected onto the band centerline at the slope q. The appropriate equation is

$$\log V_x = \frac{q}{q-s}\log V_0 - \frac{\log 2}{q-s}m - \frac{s\log V_{m_0} - m_0 \log 2}{q-s}, \quad (1)$$

where V_0 and m are the observed redshift and magnitude after standard corrections, m_0 is the reference magnitude used to define band locations ($m_0 = m_p = 15.0$ in BT), and $\log V_{m_0}$ is the band centerline location at the reference magnitude. We shall further denote X-groups by the redshift where they cross their band; thus CU65 will denote the CU X-group which crosses the CU centerline near $V_0 = 6500$ km s^{-1}.

We begin X-group analysis with an intercomparison of A1367 and Coma, using A1367 data in BT. A1367 is similar to Coma in mean redshift and should show similar structures if they are real. Figure 2 shows that this is the case. The upper panel indicates A1367 X-groups. The lower panel superposes the Coma X-group lines from Figure 1. Coma was shifted vertically (but not horizontally), because of the different magnitudes, to match the major CM X-group near $\log V_0 = 3.8$. A one-to-one correspondence of X-groups can be seen as well as the different degree of development of the low-redshift end of the band as discussed in BT.

We formally define CU X-groups by superposing Coma and A1367 in total magnitudes, as shown in Figure 3. There are now no relative shifts. Three groups are seen and are specified in the lower panel. The band line is from BT and the X-groups are shown for uniform spacing in V_0, as discussed later. Note that unlike the nuclear magnitude analysis where only galaxies within 0.3 of the Coma center could be utilized, we now include all galaxies to 0.4. Galaxies still farther out will be discussed later. Two galaxies,

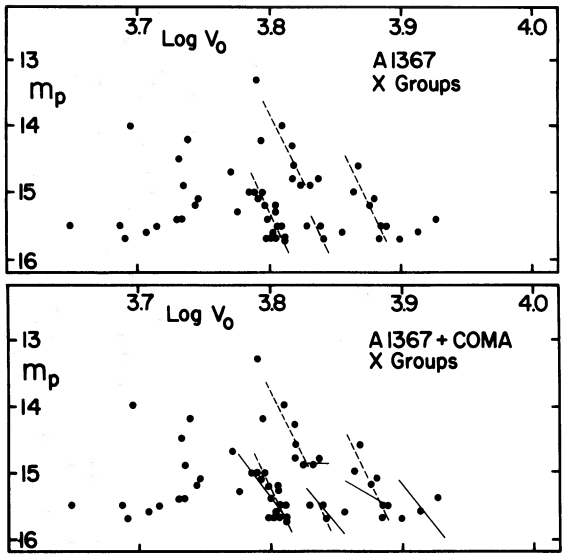

FIG. 2.—A1367 X-groups in total magnitudes. In the lower panel Coma lines from Fig. 1 are superposed to show the one-to-one redshift correspondence and the extension of development in A1367 at lower redshift.

originally assigned to the CU band by using nuclear magnitudes, associate with what appears to be a vestigial vertical sequence, and m_p magnitudes place them in the CM sample. A few such interchanges are unavoidable but have little effect, since the total samples are moderately large.

The material in Figure 3 is sufficient to demonstrate a significant CU X-group structure; however, we defer formal testing until several other clusters have been added. The most notable addition is the Perseus

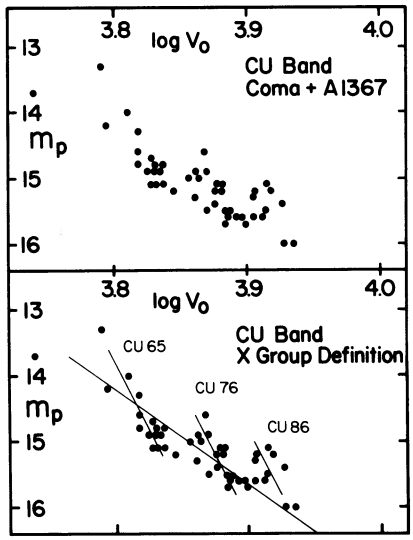

FIG. 3.—CU band X-group definition based upon a superposition of Coma and A1367 in total magnitudes. The standard CU band line is shown in the lower panel, as are three X-group definition lines.

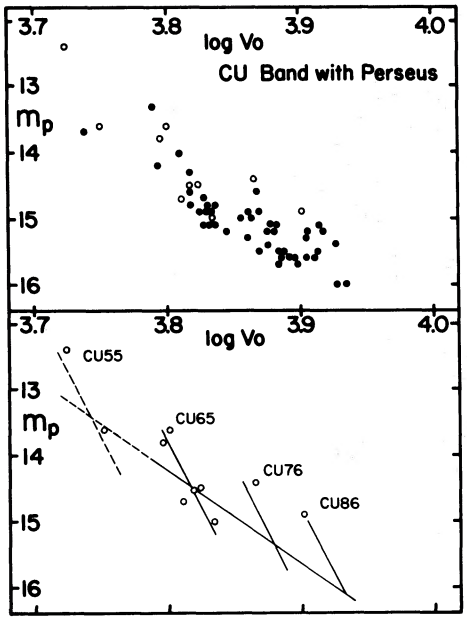

FIG. 4.—The addition of Perseus CU band galaxies (*open circles*) to the Coma + A1367 material in Fig. 3 (*filled circles*). The band is extended and a new X-group added.

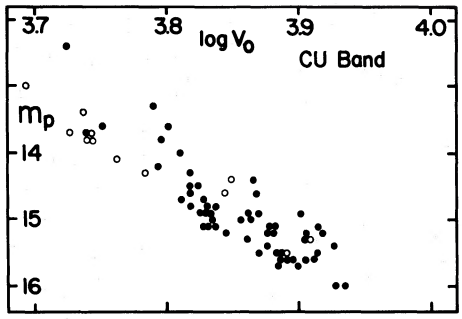

FIG. 5.—The addition of A194, A347, and NGC 507 CU band galaxies (*open circles*) to the Coma + A1367 + Perseus material in Fig. 4 (*filled circles*). Four X-groups are present.

cluster from BT, where it was shown that a significant CU population is present. Placing no restrictions on distance from the cluster center, we have 10 CU galaxies in Perseus with known m_p. We adopt the 0.6 mag absorption correction discussed in BT. Figure 4 shows the Perseus data superposed on A1367 and Coma and the band and X-group definition lines. The X-group fit is seen, as is the further progressive development of the band toward lower redshifts. A uniformly spaced (in V_0) CU55 group is added. The galaxy heading the band is the active object NGC 1275.

Three other clusters which will be major contributors to the CM band add a few CU points. They are A347 (Hintzen, Oegerle, and Scott 1978), NGC 507 (Tifft, Hilsman, and Corrado 1975), and A194 (Zwicky and Humason 1964; Chincarini and Rood 1977) which will be discussed further later. Figure 5 shows the additional contributions, most of which fall in the CU55 X-group.

Figure 6 is the V_x distribution of the 68 galaxies in the CU sample. A periodic distribution is confirmed by the power spectrum in Figure 7. A redshift periodicity near 1080 km s^{-1} is significant at the 5×10^{-4} level. It is curious, and perhaps not accidental, that the 1080 km s^{-1} interval is also the average Coma band spacing (Tifft 1974). Unlike bands, however, X-groups seem to be spaced nearly uniformly in redshift.

III. X-GROUPS AND THE CM BAND

The Coma CM band barely reaches above the magnitude limit of the CGCG catalog; hence we shall first utilize nuclear magnitude material. Figure 8 shows the CM band with the band lines defined by Tifft (1973*a*) at $s = 3.22$. The V_x projection shown was calculated at $m_0 = 16.0$, using $q = 9$. The power spectrum shown indicates a marginally significant, $p = 0.05$, periodicity in the 700–800 km s^{-1} range. The CM periodicity is distinctly less than the CU value.

We now proceed as before, combining Coma with A1367 to define the CM X-group structure in m_p. Figure 9 shows that only CM63 and the tip of CM70 extend above the CGCG limit. These two groups, along with the approximately known CM period noted above, permit estimation of the location of the next lower CM X-group. A1367 shows a few galaxies at this point but no developed group.

We now examine lower-redshift clusters, beginning with a study of A347 by Hintzen, Oegerle, and Scott (1978). The sample is incomplete but the mean redshift is centered near log $V_0 = 3.75$, which makes the cluster ideal for investigation of CM band extensions. We omit some galaxies several degrees from the cluster but utilize all other objects. We supplement the A347 sample with the total core sample of the NGC 507 cluster, a somewhat lower-redshift cluster from Tifft, Hilsman, and Corrado (1975). This sample is complete to the CGCG magnitude limit but represents only the very core of the cluster. Both A347 and NGC 507 appear to be in the Perseus supercluster (Tifft and

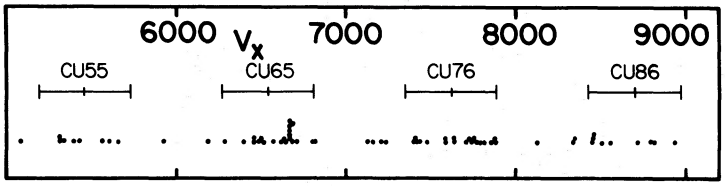

FIG. 6.—The distribution of CU band redshifts, projected to the band centerline at an X-group slope $q = 12$, for the six clusters in Fig. 5. The data are periodic as indicated.

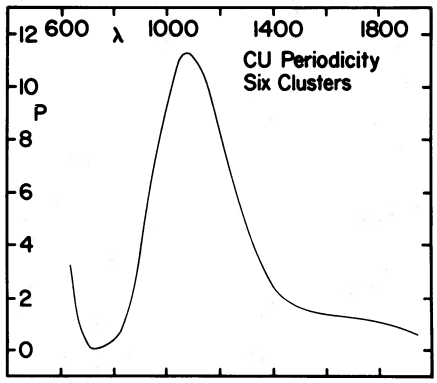

FIG. 7.—Power spectrum of the V_x distribution for the six-cluster CU composite diagram of 68 galaxies in Figs. 5 and 6. The periodicity near 1080 km s^{-1} has a 5×10^{-4} probability of occurring accidentally.

Gregory 1978). Figure 10 presents the combined sample with the clusters distinguished in the upper panel. The lower panel shows band and X-group locations, while symbols now indicate band assignments. The data agree closely with the CM63 and extrapolated CM57 X-groups, and we can easily interpret the diagram as indicative of a progressive shift of points through a fixed pattern. The CL band is now also represented, and a reference line (not an X-group line) is shown. The CL band will be briefly discussed later.

An almost ideal further sample for the CM band is available in the A194 cluster (Zwicky and Humason 1964; Chincarini and Rood 1977). We make use of the essentially complete sample within 1° of the cluster center. There is a slight inconsistency in V_0 values

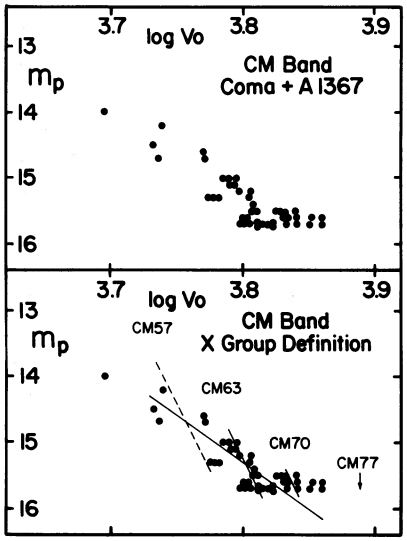

FIG. 9.—CM band X-group definition based upon a superposition of Coma and A1367 in total magnitudes. The standard CM band line is shown in the lower panel, as are X-group definition lines. The lowest-redshift group is extrapolated, and the highest-redshift group in Fig. 8 is below the CGCG magnitude limit.

between Chincarini and Rood (1977) and the RC2 (de Vaucouleurs, de Vaucouleurs, and Corwin 1976). For consistency we adopt the RC2 values and the small systematic correction given for the Zwicky and Humason redshifts in the RC2. We use Chincarini and Rood values for galaxies not in the Zwicky and Humason paper or where improved redshifts were obtained. Figure 11 shows A194 with the upper panel

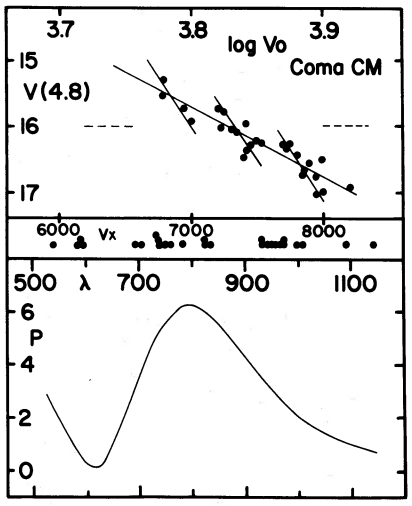

FIG. 8.—Analysis of the Coma CM band X-groups in nuclear magnitudes. The upper diagram is the basic data with the band as defined by Tifft (1973*a*). The dashed line shows the cutoff below which m_p magnitudes are unavailable. The V_x projection and the power spectrum of the V_x distribution are also shown. The V_x periodicity has a 0.05 probability of occurring accidentally.

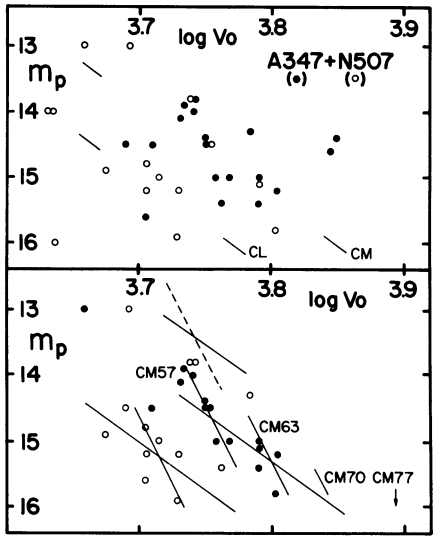

FIG. 10.—(m_p, log V_0)-diagram for the A347 and NGC 507 clusters. The clusters are distinguished in the upper panel, the band assignments in the lower panel. Standard band and X-group lines are shown for CU and CM galaxies. The line on the CL band is a reference line, not an X-group.

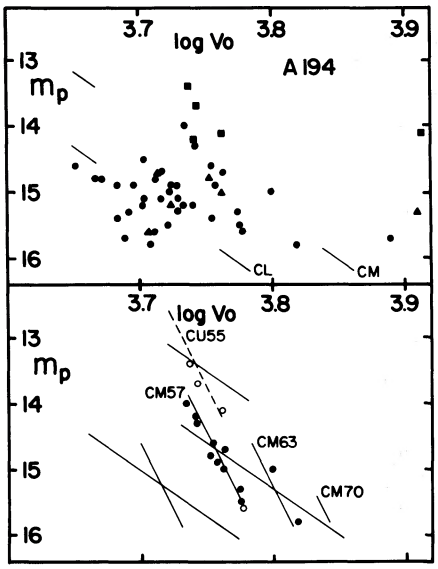

FIG. 11.—(m_p, log V_0)-diagram for the A194 cluster. The total sample to 1° is shown in the upper panel with sources indicated (*squares*, RC2; *filled circles*, Zwicky and Humason 1964 reduced according to RC2 procedures; *triangles*, Chincarini and Rood 1977). The lower panel gives band assignments and repeats lines from Fig. 10. The CL subgroup which contains two apparent X-groups is omitted in the lower panel and discussed in detail later.

indicating redshift source. The lower panel contains the predicted band and X-group lines. All the galaxies in the CU and CM regions are in close agreement with predictions. Points associating with the CL band will be discussed later.

Figure 12 is a composite diagram of A1367, A347, NGC 507, and A194 to which we add seven CM galaxies in the Perseus cluster from BT. We omit the Coma cluster to provide a completely independent sample for CM periodicity analysis. Figure 13 shows the V_x projection and Figure 14 the power spectrum. The Coma CM power spectrum is included for comparison. The five-cluster sample periodicity is significant at the 0.005 level taken alone, and at the 10^{-4} level if we take note of the period agreement of the two samples.

A common feature of all samples so far discussed is that they come from well-developed clusters. X-groups appear to be a characteristic of this stage which we hypothesize to represent an intermediate developmental stage.

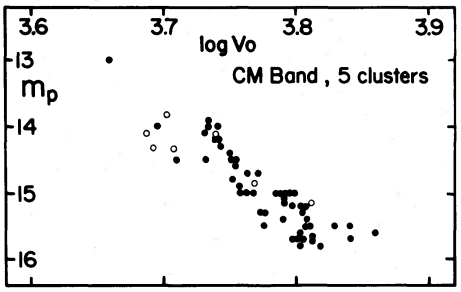

FIG. 12.—The addition of Perseus (*open circles*) to the A1367 + A347 + NGC 507 + A194 composite CM band diagram (*filled circles*). Coma is omitted to provide a test independent of the original Coma definition. Four X-groups are visible.

IV. COMPACT GROUPS

With developed band structures defined, we may now proceed either way in our hypothesized evolutionary sense. We first consider possible earlier stages by examination of compact E-dominated groups. Five such groups are known to the author which satisfy the necessary requirements of compactness, E–S0 dominance, known redshifts with redshift in the Coma range, and availability of m_p magnitudes. The five are the NGC 68 group, NGC 3158 group, and Stephan's Quintet, which are in both RC2 and CGCG, the NGC 4065 group from CS, and the Cetus group from Karachentsev and Tifft (1978). To this list we might add the IC 3481 group, although it contains only two relevant redshifts and only one galaxy has an m_p magnitude.

The above mentioned groups have two remarkable commonalities. Although they distribute widely over the sky, they superpose almost perfectly in a redshift-magnitude diagram. This is shown in Figure 15, where symbols distinguish the groups. We temporarily omit three late spirals but include all other galaxies. The five groups also have a common property of including one or more mildly "discordant redshifts." The deviation is seen to be correlated; all groups show the deviation to the low side and in similar amount, near 1000 km s^{-1}.

In Figure 16 the composite compact group diagram is repeated, with the CM and CU X-groups indicated, and is contrasted with the Coma + A1367 composite CU diagram. The diagrams are so obviously anticorrelated that no statistical demonstration is required. Two alternatives are suggested: either E-dominated compact groups and normal clusters are

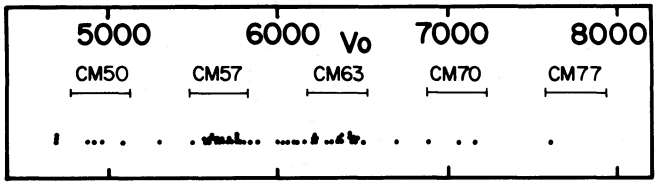

FIG. 13.—The distribution of CM band redshifts, projected to the band centerline at an X-group slope $q = 12$, for the five clusters in Fig. 12. The data are periodic as indicated.

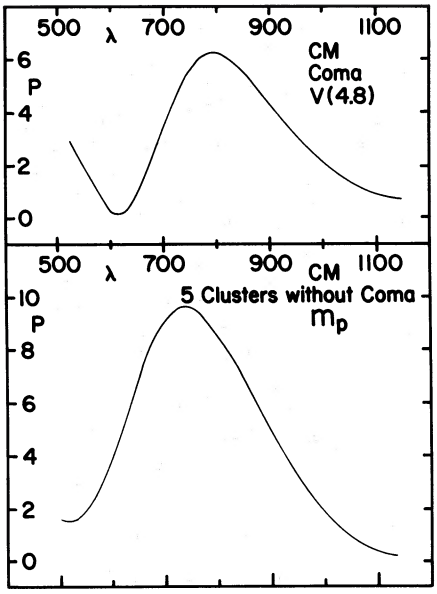

FIG. 14.—Power spectra of the original Coma CM band V_x distribution in nuclear magnitudes compared with the independent five-cluster sample of 59 galaxies in Figs. 12 and 13. Both data sets show similar periodicities. The five-cluster sample periodicity has a probability of accidental occurrence of 0.005–0.0001. The lower value takes cognizance of the period agreement.

entirely different things; or they may represent different stages in some evolutionary pattern. The clumpings at $\log V_0 = 3.85$ and 3.78–3.79 are typical BT "vertical sequences." They appear at the junctions between X-groups.

To pursue the relationship of X-groups to vertical sequences further, we can examine the vertical sequences seen in clusters, especially Perseus. It was shown in BT that the intermediate and outer parts of the Perseus cluster show strong vertical sequences (see Figs. 8 and 9 in BT). One of the strongest Perseus sequences is at $\log V_0 = 3.78$–3.79, which matches the lower-redshift compact group concentration.

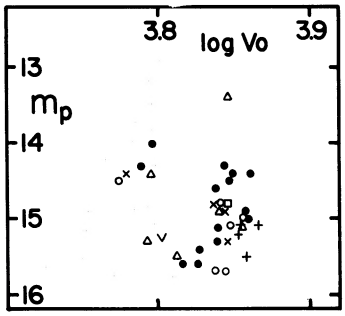

FIG. 15.—Composite (m_p, $\log V_0$)-diagram for compact E-dominated groups in the Coma redshift range. The groups are N68 (*open circles*), Stephan's Quintet (×), IC 3481 (*square*), Cetus (*fainter than and* +), NGC 4065 (*filled circles*), and NGC 3158 (*triangles*). The groups superpose to define a vertical sequence at $\log V_0 = 3.85$ and a clump of similar "discordant" objects at $\log V_0 = 3.78$–3.79. Three late spirals are not shown.

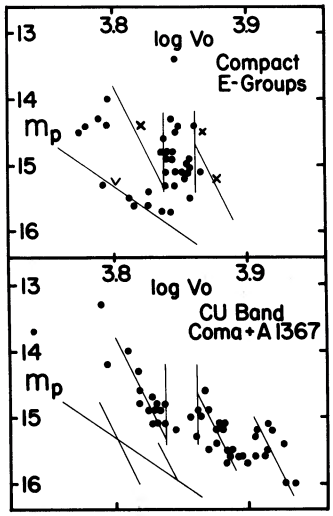

FIG. 16.—The composite compact group diagram from Fig. 15 contrasted with the Coma + A1367 X-group definition diagram from Fig. 3. X-group and standard band lines are shown and an inter-X region is defined by vertical lines. Three late spirals in the compact groups are shown with crosses. The diagrams, excepting the late spirals, are nearly perfectly anticorrelated. The "vertical sequences" in the upper panel correspond to the intervals between X-groups.

Perseus also shows a weaker clumping near $\log V_0 = 3.84$, which matches the higher-redshift sequence in the compact groups. A brief inspection is sufficient to demonstrate in general that cluster vertical sequences occur *between* X-groups. Figure 17 schematically summarizes the compact group and cluster material.

In the framework of an evolutionary hypothesis we can infer that injection occurs at unique redshifts which correspond to junctions between X-groups. Subsequent evolution can then be assumed to shift the galaxies into the X-group domains. In this context we note that the three crosses in Figure 16 represent the three late-type spirals in the compact groups. They populate the X-group regions, not the regions between. In our evolutionary hypothesis, late spirals are the most advanced objects. Another possible

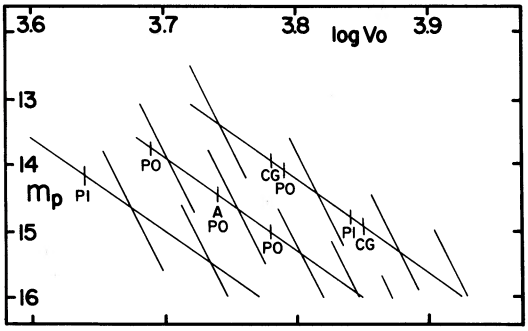

FIG. 17.—Summary of bands and X-groups showing the locations of the more prominent vertical sequences. CG = compact groups, PO = Perseus outer, PI = Perseus intermediate, A = A1367. The vertical sequences appear to be limited to inter-X regions and correspond in different samples.

indication in Figure 16 comes from noting that one of the two Coma ellipticals which falls in the inter-X region (IC 3959 at $\log V_0 = 3.85$, $m_p = 15.2$) is a member of Coma β (Tifft 1972), which is a compact subcluster within Coma. This galaxy is therefore a candidate for association with the compact groups.

V. MORPHOLOGICAL CORRELATIONS

To pursue evolutionary concepts further, we now consider diffuse populations which we hypothesize to represent advanced stages. We make use of the outer Coma data of Tifft and Gregory (1976) and isolated Coma supercluster galaxies from Gregory and Thompson (1978). One essential ingredient which has been missing previously is accurate morphology for outer Coma galaxies. This has been rectified by classifying all CGCG galaxies within 1°, and ones farther out when possible, using KPNO 4 m negatives (the author wishes to express his appreciation to S. A. Gregory and L. A. Thompson for use of film copies of their plates). The classification was done visually by the author and is listed in Table 1. Most galaxies in the central field already have good classifications (Rood and Baum 1967) and were not repeated. Each galaxy is identified by CGCG number which can be cross-referenced to other names via Tifft and Gregory (1976). Classification was done before any statistical analysis was considered and no subsequent revisions were made.

We begin by dividing the Coma data into radial zones. One boundary is at 1°, where morphological incompleteness begins. Other boundaries are at 0°.25 and 2°.1, where changes in the redshift distribution appear to occur as shown in Figure 18. Within 0°.25 we find nearly all the very high- and low-redshift objects, and very few galaxies of type later than S0. A marked concentration appears between $\log V_0 = 3.82$ and 3.84. Rather suddenly at 0°.25 the high- and low-redshift objects vanish and a distinct gap appears

TABLE 1

COMA MORPHOLOGY

Zwicky	Type	Zwicky	Type	Zwicky	Type
160A 1	S0	160 37	SB0	160 79	Sab
2	S0	39	E2	81	S0/a
5	SB0	40	E4	83	S0
6	E2	42	E1	85	E3
8	E0	43N	S0/a	86	I/Sc
160A 31	E7/S0	160 44W	E1	160 87	S0
40	S0/a	44E	E0	89	E/S0
42	Sb:	46S	S0	90	Sab
48	SBb	46N	E1	91	S0
51	Sc	47	Sa	92	E/S0
160A 52	Sa	160 48W	S0	160 93	S0
159 85	S0/E7	48E	S0	94	S0/a
87	SB0	49N	S0	95	SBb
90	SBbc	51	S0/a	97	E2
93	Sbc	52	S0	98	Sc
159 94	SBab	160 53	E/S0	160 100	E1
97	Ip(R)	55	Sc	101	S0
99	Sbc	57	S0	103	E1
101	IrII	58	Scp	104	S0/a
104	Sc	59	E7/S0	105	E3
159 111	S0/a:	160 61S	SB0	160 106	Sbp
112	Sc	61N	SB0	108	I/Sc
113	E	62N	S0:	109	SB0
118	S0p/a	62S	Sc:	110	S0
160 15	Sa	63	S0:	111	E/S0
160 17	E	160 64	Sp	160 112E	S0/a
18	S0/a	65	E1	113	E2
19	E/S0	66	S0	114	Sab
20	I	67	I/Sc	115	E/S0
21	E2	68	S0	116	S0
160 23	E0-1	160 69	S0/a	160 118	S0
24	S0	70	E2	119	E7/S0
25	Sb	71	Sa	120	Sb:
26	Scd	73	Sp	122	S0
27	E0	74	SB0	123	E0
160 28	E	160 76	I/Sc	160 124W	S0
29	S0	77	S0	124E	SB0
31	Sbp	78	S0	125	S0

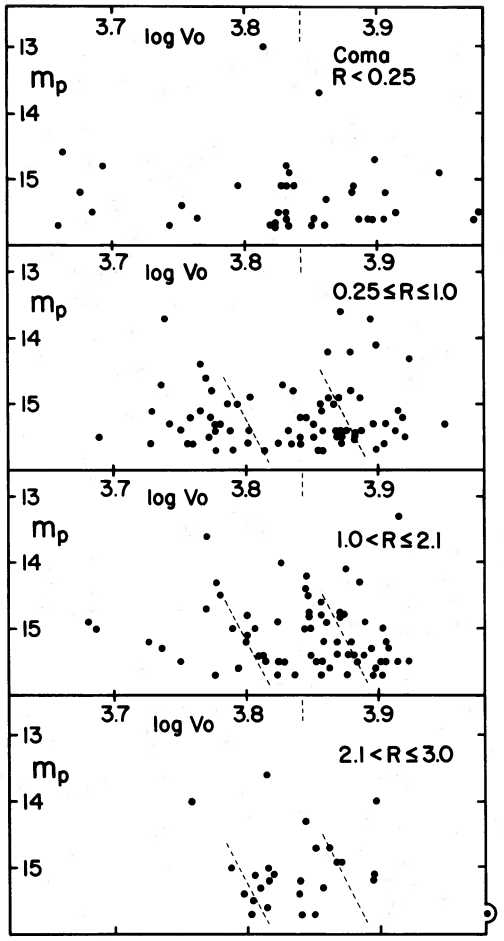

FIG. 18.—Coma (m_p, log V_0)-diagrams separated by radial groups. The core redshift distribution becomes bimodal farther out with the two groups relating to specific X-groups as shown, CM63 and CU76.

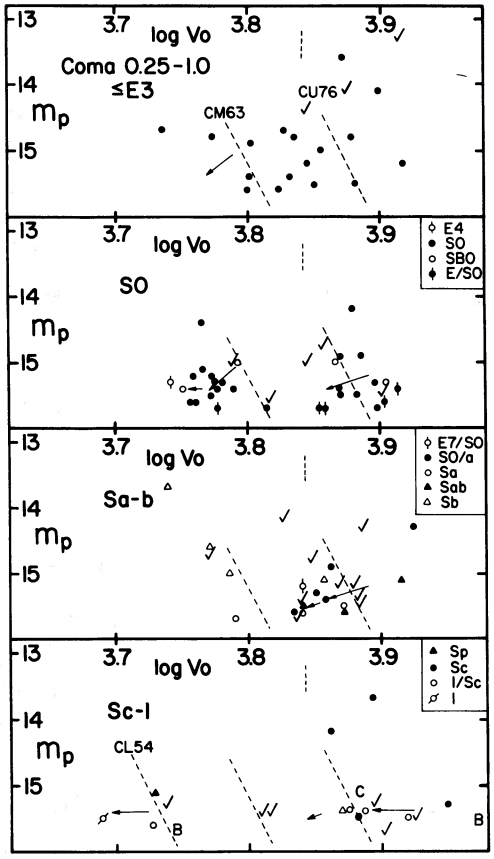

FIG. 19.—Coma (m_p, log V_0)-diagrams for R between 0°.25 and 1°.0 separated by morphology. Galaxies with R greater than 1°.0 are shown with check marks and, three late spirals in the core appear in the last panel with B or C to indicate types. The cluster mean redshift is shown with a dashed vertical line. Several X-groups are indicated and vectors copied from frame to frame are used to map population shifts.

where the central concentration was seen. The distribution becomes distinctly bimodal, each clump associating with a particular band and X-group. A comparison of numbers in and out of the log V_0 = 3.82 to 3.84 interval demonstrates the change. The in:out ratio changes from 12:28 to 5:69 and remains low at all outer radii. Similar changes may occur in other redshift ranges. The redshift clumping is not related to position within the circular rings, nor is it symmetrical about the cluster mean redshift indicated at the top of each panel. At larger radii the duality persists with a progressive shift toward the X-group centerlines in both redshift and brightness. We now examine the clumps and shifting patterns for morphological trends which might relate to evolutionary concepts.

We divide the galaxies into four morphological subclasses, the least flattened ellipticals, the flattened ellipticals and S0 or SB0 types, the lenticulars E7/S0 and early to middle spirals, and the late spirals and irregulars. Figure 19 presents the 0°.25–1°.0 sample broken down by type. Classified galaxies at greater radii are also shown with a separate symbol. The redshift distribution for each subclass is entirely different. The ellipticals show no evidence of the bimodal pattern. Except for a few additions in the CM63 region they extend the higher redshift pattern of the center. The bimodal pattern stands out sharply in the S0 subgroup. Clumps fall at the outer edges of the ellipticals and no galaxies fall in between. The clumping has been noted previously (Tifft 1974), using older independent morphological types. The lower group virtually disappears in the early spirals, while the upper group shows a distinct shift. The pattern shifts and changes again with the late spirals. The CM63 X-group can be traced from a few ellipticals close to the definition line through the distinctly shifted S0 group and possibly into the late spirals. A simple morphological ordering is present in descending order from the CM63 X-group definition line. Likewise the CU76 group shows a smooth trend passing from the S0 types to early spirals. The late spirals suggest two separate groups for which no earlier types

are seen, although the lower group could associate with the CM63 clump. The limited outer data confirm the basic features.

One remaining point is the relationship of outer Coma to inner Coma. Figure 19 shows two definite morphological sequences which end near $\log V_0 = 3.75$ and 3.84. If we consider the late-type galaxies to define two additional sequences, then there are also endpoints near $\log V_0 = 3.70$ and 3.90. This set of four sequences corresponds to one from each band from CL through Q6. A still higher sequence could be present near $\log V_0 = 3.97$. Vectors marking the extent of the sequences are shown in Figure 19. Figure 20 shows that the tips of these vectors relate directly to the redshift location of the galaxies in the core. Morphologically, however, the core is different; the core galaxies are predominantly early, whereas it is late-type galaxies outside the core which define the sequences. There appears to be a transition on each sequence from late to early type as one enters the core. There is one further relationship, however; the core galaxies associate with the lower right end of the next X-group on each band starting from the X-group where each morphological sequence originates. The morphological sequences therefore *link* X-groups. A new possibility must thus be considered. Emergence may conceivably not be from new singularities, it may be from *recycled* galaxies.

The outer Coma morphological patterns are in themselves quite significant; however, the best test of any concept comes from independent samples. Several are available. In A194, shown in Figure 11, a diffuse clump of galaxies appears on the CL band. Two sets of morphological classifications, tabulated by Chincarini and Rood (1977), are available for these galaxies. Figure 21 shows the A194 CL material separated morphologically. The same morphological trend seen in Coma is present, linking two possible X-groups (shown dashed). The limited low-redshift material in A1367 is also plotted and shows the same trend. A formal test of the shift can be made by comparing the numbers of galaxies on either side of a reference line shown. The numbers are given in the figures and the shift is significant.

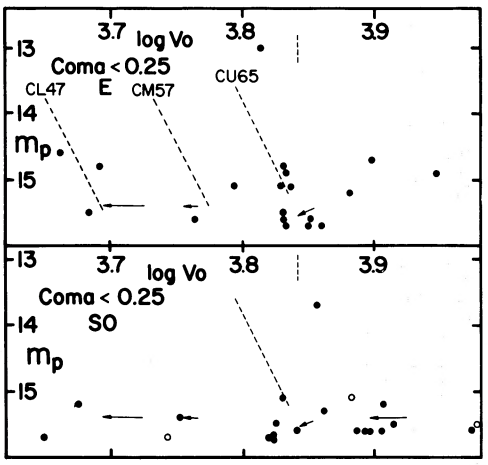

FIG. 20.—Coma (m_p, $\log V_0$)-diagrams for the cluster core separated by morphology. The three late-type galaxies in the core are shown with open circles. Markings are similar to Fig. 19 except the next lower set of X-groups is shown. The most advanced morphological sequence vectors from Fig. 19 are also indicated, and correspond with the galaxy redshift distribution in the core. Note the slight further progressive shift in the core when going from E to S0 types.

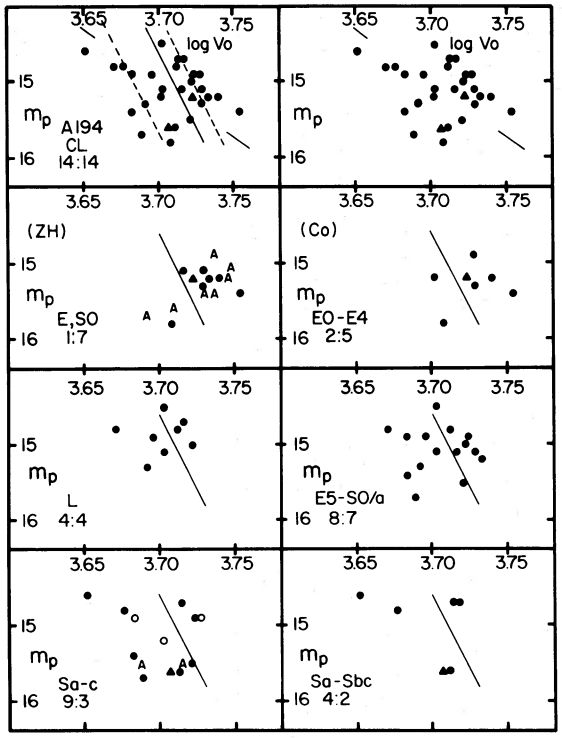

FIG. 21.—Morphological sorting in the CL region of A194. The upper panels show the complete CL subgroup, on the left with two possible X-groups (*dashed*) and a reference line which evenly divides the population. In the lower panels the population is separated morphologically according to Zwicky and Humason (ZH) types or Corwin (Co) types as given by Chincarini and Rood (1977). Ratios between the sides of the reference line are given. Low-redshift data from A1367 are also shown with A symbols. The same morphological shift seen in Coma is present in both A194 and A1367.

A further example is available by using the Coma supercluster isolated component from CS. Figure 22 shows the brighter sample for which good morphology is available. The CU65 X-group region is well populated. The E/S0 population is dominant above the X-group reference line, the late spirals below. The scattered higher-redshift late spirals are consistent if we interpret them as the last remaining stage of still higher-redshift X-groups much as the high-redshift late component persists in Coma. The X-group linkage and morphological sequences are significant and found in all samples.

VI. DISCUSSION

Redshift-magnitude bands contain a significant X-group structure at slope $q \approx 12$ in total magnitudes.

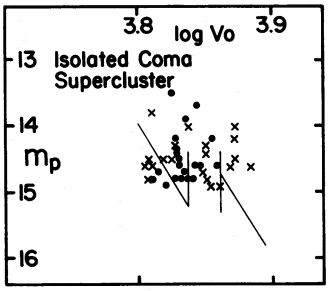

FIG. 22.—The isolated Coma supercluster sample with m_p brighter than 15.0 from CS. The CU reference X-group and inter-X lines from Fig. 16 are shown. The morphological shift across the CU65 X-group is visible. Note that the E galaxy population concentrates at the same redshift as the Coma core E galaxies in Fig. 18.

TABLE 2

X-GROUP BAND CROSSING POINTS

Group	log V_x	Group	log V_x
CU55.....	3.742	CM63.....	3.802
CU65.....	3.816	CM70.....	3.845
CU76.....	3.879	CM77.....	3.884
CU86.....	3.933	CL47.....	3.675
CM50.....	3.703	CL54.....	3.735
CM57.....	3.756		

Table 2 lists the band crossing points assumed in this paper. The groups appear to be more or less uniformly spaced in redshift with crossing points 700–1100 km s^{-1} apart, depending upon the band involved. The groups appear to be linked together by sequences of galaxies showing a Hubble sequence morphological trend. The sequences make precise definition of X-groups somewhat difficult; hence the Table 2 values should be taken as approximations dependent upon morphology and the type of galaxy aggregates used.

Preliminary evolutionary band theory in BT can be modified to accommodate the new observations. An evolutionary track showing progressive redshift as well as luminosity drift is conceivable. By recognizing that multiple cycles are operating simultaneously, apparently in synchronization, it is possible to explain the presence of some low-redshift spirals as well as the general trend toward high-redshift spiral dominance. Further, we now recognize the possibility that the vertical sequences of BT may represent recycling points for galaxies entering X-groups rather than completely new emergence. The concept of rapidly converting a late spiral into an elliptical poses obvious difficulties. The one-to-one correspondence of outlying late spiral and core elliptical redshifts is, however, an empirical fact, and time evolution appears to be the only mechanism that can explain the types of correlations observed. Examples are known, NGC 5128 for example, where early and late types are mixed; hence the hypothesis is made pending further study.

REFERENCES

Chincarini, G., and Rood, H. J. 1977, *Ap. J.*, **214**, 351.
de Vaucouleurs, G., de Vaucouleurs, A., and Corwin, H. G. 1976, *Second Reference Catalogue of Bright Galaxies* (Austin: University of Texas Press) (RC2).
Gregory, S. A., and Thompson, L. A. 1978, *Ap. J.*, **222**, 784.
Hintzen, P., Oegerle, W., and Scott, J. 1978, *A.J.*, **83**, 478.
Karachentsev, I., and Tifft, W. G. 1978, *Astr. Ap.*, **63**, 411.
Rood, H. J., and Baum, W. A. 1967, *A.J.*, **72**, 398.
Tifft, W. G. 1972, *Ap. J.*, **175**, 613.
———. 1973*a*, *Ap. J.*, **179**, 29.
———. 1973*b*, *Ap. J.*, **181**, 305.
———. 1974, *Ap. J.*, **188**, 221.
———. 1978*a*, *Ap. J.*, **221**, 756.
Tifft, W. G. 1978*b*, *Ap. J.*, **222**, 421 (BT).
Tifft, W. G., and Gregory, S. A. 1976, *Ap. J.*, **205**, 696.
———. 1978, in *IAU Symposium No. 79, Large-Scale Structure of the Universe*, ed. M. S. Longair and J. Einasto (Dordrecht: Reidel), p. 267.
———. 1979, *Ap. J.*, **231**, 23 (CS).
Tifft, W. G., Hilsman, K. A., and Corrado, L. C. 1975, *Ap. J.*, **199**, 16.
Zwicky, F., Herzog, E., Wild, P., Karpowicz, M., and Kowal, C. 1960–1968, *Catalogue of Galaxies and Clusters of Galaxies*, 6 vols. (Pasadena: California Institute of Technology Press) (CGCG).
Zwicky, F., and Humason, M. L. 1964, *Ap. J.*, **139**, 269.

WILLIAM G. TIFFT: Steward Observatory, University of Arizona, Tucson, AZ 85721